Domain of attraction for stabilized orbits in time delayed feedback controlled Duffing systems

Kohei Yamasue and Takashi Hikihara
Department of Electrical Engineering, Kyoto University, Nishikyo, Kyoto 615-8510, Japan
(Received 20 June 2003; published 17 May 2004; publisher error corrected 28 May 2004)

Time delayed feedback control is well known as a practical method for stabilizing unstable periodic orbits embedded in chaotic attractors. However, this control method still has an open problem of estimating domain of attraction for target unstable periodic orbits. In this paper, we numerically discuss the domain of attraction in Duffing systems under the control method. The disturbance to initial conditions reveals that the domain of attraction possibly exhibits self-similar structures in its boundaries.

DOI: 10.1103/PhysRevE.69.056209 PACS number(s): 05.45.Gg

I. INTRODUCTION

Controlling chaos has become an energetic research field in nonlinear science in this decade [1]. The key concept proposed by Ott, Grebogi, and Yorke [2] has highly motivated researchers to devise and develop several advanced methods for stabilizing unstable periodic orbits embedded in chaotic attractors. Among them, the time delayed feedback control, proposed by Pyragas, is endowed with crucial advantage for control of practical chaotic systems [3]. Without any exact model of controlled objects and complicated computer processing for reconstruction of underlying dynamics, the method can stabilize target unstable periodic orbits by using the difference between present output signals and past ones. So far, the control method has been experimentally examined in diverse research areas : electronic circuits [4], laser systems [5], mechanical oscillators [6], chemical systems [7], and so on. Moreover, the control mechanism has been theoretically studied on the basis of linearization technique (see Ref. [8] and references therein). One of the notable results is referred to as the odd number condition. The odd number condition gives a class of unstable periodic orbits which the control method and its extension [9] cannot stabilize. The odd number condition was first proved for discrete systems [10] and subsequently extended to continuous systems [11,12]. Against this negative result, Pyragas has recently improved the control method to overcome the odd number condition [13].

On the other hand, there still remain open problems for clarification of the control performance [8]. One of them is the estimation of the domain of attraction for the target unstable periodic orbits. The estimation of the domain of attraction is indispensable for the application of the control method. The largeness and structure of the domain of attraction is closely related to the practical problems such as deciding onset timing of control and estimating the effect of noise. However, the estimation of the domain of attraction is hard to tackle owing to the following two reasons. One reason is that, in general, the domain of attraction is closely linked with global dynamics of controlled systems. Thus, the problem is obviously beyond the scope of linearization in the neighborhood of the target unstable periodic orbits. The other is that the domain of attraction exists in function space and then in infinite dimensional space under the control method. This characteristic comes from the time delay included in the feedback loop [14]. Despite these intractable properties, study on the domain of attraction is essential for engineering use of the control method.

In this paper, we numerically discuss the domain of attraction in the Duffing systems under the control method. This paper deals with two types of Duffing systems exhibiting chaos under certain parameter regions. These Duffing systems are here considered as a model of the magnetoelastic system [15] or hard symmetric spring in a mechanical system [16]. The controlling chaos of Duffing systems is an important subject of research in engineering field, since it is relevant to elimination of the chaotic vibration in these mechanical systems.

This paper consists of the following sections. Section II describes mathematical representation of the time delayed feedback controlled Duffing systems. The above two types of Duffing systems are introduced as controlled objects with scalar input and output. The control method is implemented to these Duffing systems with use of velocity feedback or displacement one. Section III systematically investigates the dependence of stabilized states on initial conditions in function space. The investigation is performed in a parameter plane concerning onset time of control and feedback gain. In Sec. IV, the structure of the domain of attraction is discussed in function space. The boundaries of the domain of attraction are examined with additional disturbance to initial conditions selected from chaotic trajectories.

II. DUFFING SYSTEM WITH TIME DELAYED FEEDBACK CONTROL

The Duffing systems are two-dimensional nonautonomous systems originating in a model of synchronous machines [17]. The two types of Duffing systems are here treated as a model of the magnetoelastic beam system [15] or hard symmetric spring in a mechanical system [16].

This section first gives general description of the time delayed feedback controlled Duffing systems. The Duffing systems coupled with a scalar control input are given as follows:

$$\frac{\mathrm{d}}{\mathrm{d}t}\begin{bmatrix} x \\ y \end{bmatrix} = \begin{bmatrix} y \\ -\delta y + \alpha x - \gamma x^3 + A\cos\omega t \end{bmatrix} + \boldsymbol{b}u, \qquad (1)$$

where x and y denote the displacement and velocity of Duffing systems, respectively. u is control signal and $\boldsymbol{b}$ two-dimensional vector concerning coupling of the control signal.

In the time delayed feedback control, the control signal is determined without any information of the target orbits except their governed periods. The control signal is simply given by the difference between present output signal and past one:

$$u=\begin{cases}0;(0\leqslant t<t_0)\\ K[g(x_\tau,y_\tau)-g(x,y)];(t\geqslant t_0),\end{cases} \tag{2}$$

where K is feedback gain and t_0 is onset time of control. The $g(x,y)=g(x(t),y(t))$ and $g(x_\tau,y_\tau)=g(x(t-\tau),y(t-\tau))$ imply present and past scalar output signals, respectively. The τ is time delay, which is adjusted to the period of a target unstable periodic orbit embedded in a chaotic attractor. This simple control strategy is easily implemented to experimental systems without exact models of controlled objects and reconstruction of underlying dynamics from experimental data. The control signal converges to null when the system is stabilized at one of the target orbits. As a result of this convergence, the controlled system degenerates from the infinite dimensional system with time delay to the original two-dimensional system without time delay. Note that the domain of attraction for target orbits is characterized by the infinite dimensional space under remarkable control input. Thus, the estimation of the domain of attraction goes beyond the scope of linearization in the neighborhood of the original system.

The onset time of control is a substantial control parameter, which determines the initial conditions of the controlled system. The initial condition at t_0 consists of the following initial values and initial function:

$$x(t_0)=x_{t_0},$$

$$y(t_0)=y_{t_0},$$

$$u_{t_0}(t)=K[g(x_\tau,y_\tau)-g(x,y)];t\in[t_0-\tau,t_0]. \tag{3}$$

In this paper, we identify the initial condition with a segment of the chaotic trajectory $[x(t),y(t)]^T;\ t\in[t_0-\tau,t_0]$ generated by Eq. (1) under $u(t)=0$. The reason is a specific initial condition described as Eq. (3) is essentially transformed from the segment of the chaotic trajectory through Eq. (2) without loss of generality.

The implementation of the control method is specifically described by the coupling $\boldsymbol{b}$ and output signal $g(x,y)$. Two simple types of implementation are introduced here. One is *velocity feedback control* specially given by replacing $\boldsymbol{b}$ with $[01]^T$ and $g(x,y)$ with y in Eq. (1). The velocity feedback control employs the velocity component for the control signal. The other is *displacement feedback control* represented by Eq. (1) under $\boldsymbol{b}=[10]^T$ and $g(x,y)=x$. The displacement feedback control uses the displacement component for the control signal.

In this paper, two types of Duffing systems are treated as for the controlled objects. In the following discussion, one is referred to as *two-well Duffing system* and the other is simply called *Duffing system*. The two-well Duffing system is a model for the first-mode vibration in magnetoelastic beam system with sinusoidal forcing [15]. The two-well Duffing system is given by Eq. (1) at $(\alpha,\gamma)=(1.0,1.0)$. The details of the dynamics under $\omega=1.0$ was discussed in Ref. [18]. The stabilization of chaos in the magnetoelastic beam system was experimentally achieved with velocity feedback control [6]. The feature of the phase propagation of the control signals was discussed in Ref. [19]. The Duffing system is a model for a hard symmetric spring in a mechanical system [16]. The Duffing system is described by Eq. (1) under $(\alpha,\gamma)=(0,1.0)$. The dynamics under $\omega=1.0$ was summarized in Ref. [16]. In Eq. (1), x and y denote the displacement and velocity of mechanical vibration, respectively, δ is damping coefficient. A indicates forcing amplitude and ω denotes its frequency. In the following sections, the system parameter (δ,A) is fixed at the values where the Duffing systems generate the chaotic attractors under $\omega=1.0$ [16,18]. τ is adjusted at 2π for stabilizing two symmetric period-2π unstable periodic orbits embedded in each chaotic attractor. It is easily confirmed that both velocity feedback control and displacement feedback control can stabilize the two symmetric period-2π target orbits under certain ranges of feedback gain. However, systematic design of feedback gain still remains another open problem in the control method [20].

III. INITIAL CONDITION

An initial condition is selected from a segment of the chaotic trajectory generated by Eq. (1) under $u(t)=0$. In this section, the dependence of stabilized states on initial conditions is discussed.

Initial conditions vary with onset time of control because of chaotic motion of original systems. It implies that onset time of control is a substantial control parameter to determine initial conditions. Then the convergence characteristics concerning onset time give crucial information of the dependence on initial conditions. When the control starts at onset time t_0 under feedback gain K, the initial condition is determined with relation to a point in (t_0,K) surface, as illustrated in Fig. 1(a). The (t_0,K) surface runs along the chaotic trajectory and is extended in the direction of K axis. The classification of points in the (t_0,K) surface with stabilized states enables the systematic investigation of the dependence on initial conditions. Figure 1(b) is a schematic diagram of a (σ_0,K) plane which covers the (t_0,K) surface over the θ_0th period with respect to the sinusoidal external force. Here θ_0 is a non-negative integer. σ_0 denotes the onset phase governed by the sinusoidal forcing and then is included in $[0,\tau)$.

Figure 2 shows (σ_0,K) planes in the two-well Duffing system with velocity feedback control. Figure 2(a) is obtained at $(\delta,A)=(0.3,0.34)$. Figure 2(b) corresponds to $(\delta,A)=(0.16,0.27)$. Figure 2(c) shows the classification of tones. This classification does not distinguish periodic states which have the same period. In Figs. 2(a) and 2(b), there is a dominant region in which the state converges to the target period-τ orbits. However, convergence to other periodic orbits often occurs at several values of feedback gain. For ex-

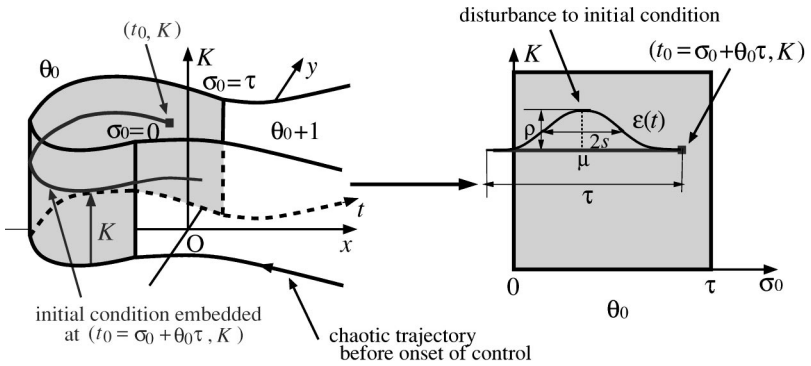

FIG. 1. A schematic diagram of initial condition embedded into onset time and feedback gain parameter plane. Surface in (a) displays chaotic trajectory generated by uncontrolled system; the surface is extended in the direction of feedback gain axis. Initial condition yielded at onset time t_0 under feedback gain K is related to a point (t_0,K) in the surface. (b) shows (σ_0,K) plane which covers (t_0,K) surface from $t_0=\theta_0\tau$ to $t_0=(\theta_0+1)\tau$ where θ_0 is non-negative integer and σ_0 is included in $[0,\tau)$. Gaussian-like curve in (b) shows schematic diagram of external disturbance $\boldsymbol{\varepsilon}(t)$ employed for disturbing initial condition in function space.

ample, one clearly recognizes the convergence to period-3τ orbits at $K\approx 0.935$ or period-6τ orbits within $0.9\lesssim K\lesssim 0.93$ in Fig. 2(a). In Fig. 2(b), one easily observes the convergence to period-6τ orbits in $1.015\lesssim K\lesssim 1.035$ or period-12τ orbits at $K\approx 1.01$. These periodic orbits coexist with the target orbits under control signal. These *coexisting orbits* become stable within ranges of feedback gain inherent to each coexisting orbit. The same results are also obtained for variety of selected spans of the onset time of control, although the presented figures do not cover the whole span. Once the controlled system converges to stable coexisting orbits, some external operation is needed to change the state of the controlled system to the target states. Therefore, the convergence to coexisting orbits implies the failure of control as a concept of controlling chaos.

Note that there is a difference in the distribution of initial conditions toward the coexisting orbits. In Fig. 2(a), initial conditions of this kind of cluster within $0.9\lesssim K\lesssim 0.935$. The

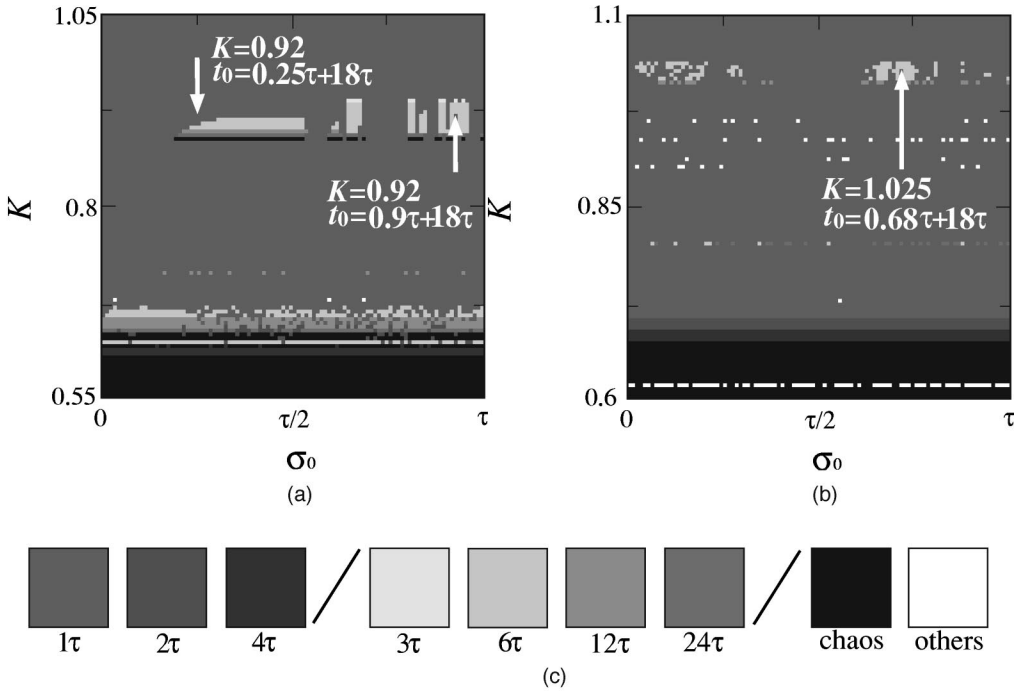

FIG. 2. Classification of stabilized orbits in onset time and feedback gain parameter plane. (a) and (b) are obtained for the two-well Duffing system with velocity feedback control at $(\delta,A)=(0.3,0.34)$ for $\theta_0=18$ and $(0.16,0.27)$ for $\theta_0=18$, respectively. (c) displays classification of tones which distinguishes period of stabilized orbits. In (a) and (b), convergence to coexisting orbits is found in particular values of feedback gain. Each point indicated by arrow corresponds to initial condition and value of feedback gain used in calculation of Fig. 5(a): $(t_0,K)=(0.25\tau+18\tau,0.92)$, Fig. 5(b): $(0.9\tau+18\tau,0.92)$, and Fig. 6: $(0.68\tau+18\tau,1.025)$. The same classification of tones is used in Figs. 3, 4, and 9(a) again.

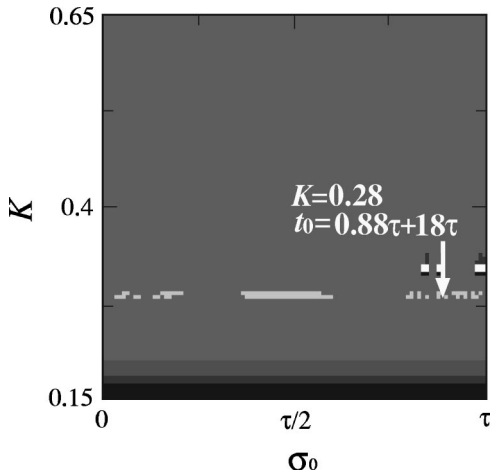

FIG. 3. Classification of stabilized orbits in onset time and feedback gain parameter plane. The classification is obtained for two-well Duffing system with displacement feedback control at $(\delta,A)=(0.46,0.4)$ for $\theta_0=18$. The classification of tones is displayed in Fig. 2(c). Convergence to coexisting period-6τ orbits appears around $K=0.28$. Initial condition corresponding to indicated point $(t_0,K)=(0.88\tau+18\tau,0.28)$ is used in calculation of Fig. 7.

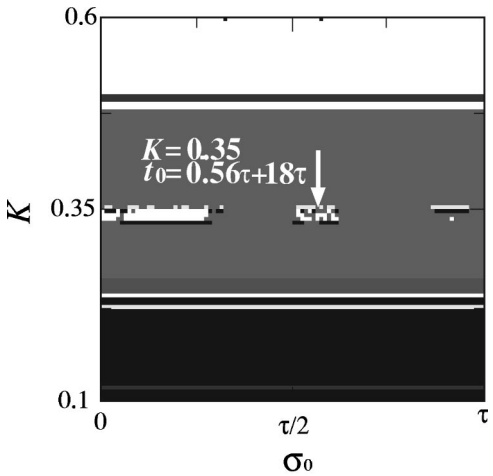

FIG. 4. Classification of stabilized orbits in onset time and feedback gain parameter plane. The classification is obtained for Duffing system with velocity feedback control at $(\delta,A)=(0.1,13.3)$ for $\theta_0=18$. The classification of tones is displayed in Fig. 2(c). Convergence to coexisting period-3τ orbits is observed around $K=0.35$. Initial condition corresponding to point $(t_0,K)=(0.56\tau+18\tau,0.35)$ indicated by arrow is used in calculation of Fig. 8.

clustering distribution suggests the small shift of the initial condition does not cause the change of the stabilized state. In contrast, initial conditions of the above kind scatter within $1.015 \lesssim K \lesssim 1.035$ in Fig. 2(b). The scattering distribution implies stabilized states alternate between the target orbits and coexisting ones, sensitively depending on small change of the initial condition. Therefore, the difference between the clustering and scattering distribution reflects the difference in sensitivity of the dependence on initial conditions.

The convergence to coexisting orbits are also recognized, even when the displacement feedback control is implemented. Figure 3 shows a (σ_0,K) plane in the two-well Duffing system with displacement feedback control at $(\delta,A)=(0.46,0.4)$. There are many initial conditions toward coexisting period-6τ orbits at $K\approx 0.28$. The clustering distribution of initial conditions is observed around $\sigma_0=\tau/2$. The scattering distribution is also found around the initial condition pointed in Fig. 3. Note that both velocity feedback control and displacement one are implemented without any dependence on specific information of the two-well Duffing system. Therefore, one can at least conjecture that the convergence to coexisting orbits is not limited to particular implementation of the control method.

Furthermore, it can be confirmed that convergence to coexisting orbits occurs, when the controlled object is replaced with the Duffing system. Figure 4 is a (σ_0,K) plane in the Duffing system with velocity feedback control at $(\delta,A)=(0.1,13.3)$. Initial conditions toward coexisting period-3τ orbits are observed at $K\approx 0.35$. The clustering distribution is found around $\sigma_0=0.9\tau$. The scattering distribution is also seen around an initial condition pointed by arrow in Fig. 4. Thus, convergence to coexisting orbits is not specific to the two-well Duffing system. Taking account of the previous conjecture, we suggest that convergence to coexisting orbits does not necessarily depend on particular implementation of the control method and specific controlled objects.

In this section, the dependence of stabilized states on initial conditions has been discussed. The investigation shows the possibility of the convergence to coexisting orbits. This convergence characteristics must be directly related to structures of the domain of attraction. In the following section, we are going to investigate the structure of the domain of attraction in function space.

IV. DOMAIN OF ATTRACTION

Once an initial condition is selected, the control with constant feedback gain uniquely achieves the convergence to an orbit. Then the systematic estimation of the effect of external disturbance on the convergence gives us substantial information of the domain of attraction in function space. Here the external vector disturbance $\boldsymbol{\varepsilon}(t)=[\varepsilon(t),\dot{\varepsilon}(t)]^T$ is additionally given to an initial condition. $\varepsilon(t)$ is represented as follows:

$$\varepsilon(t)=\rho\exp\left\{-\left(\frac{t-\mu}{s}\right)^2\right\}, \tag{4}$$

where t and μ are included in $[t_0-\tau,t_0]$, t_0 denotes onset time of control. In the following discussion, s is fixed at $\tau/2$, which determines the distribution of the external disturbance. ρ is a non-negative value sufficiently smaller than the amplitude of the motion of Duffing systems. ρ implies the intensity of the external disturbance. μ defines the center of the distribution along temporal axis. The disturbance $\boldsymbol{\varepsilon}(t)$ is physically interpreted as a small impact force externally given to the mechanical oscillator in a period just before onset of control. The disturbance is evaluated at every center of impact μ with introduction of the $(\mu,\|\boldsymbol{\varepsilon}(t)\|_\tau)$ space. The $\|\boldsymbol{\varepsilon}(t)\|_\tau$ denotes L^2 norm of $\boldsymbol{\varepsilon}(t)$.

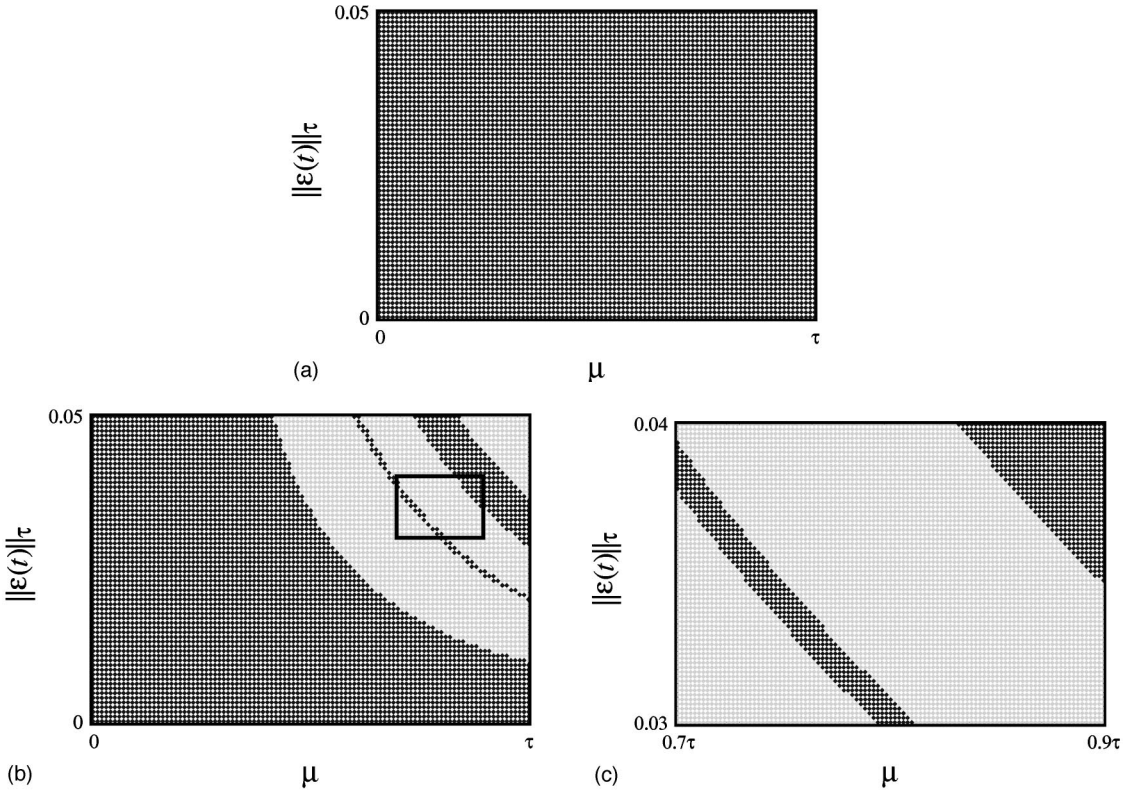

FIG. 5. Domains of attraction on $(\mu,\|\boldsymbol{\varepsilon}(t)\|_\tau)$ space in two-well Duffing system with velocity feedback control at $(\delta,A)=(0.3,0.34)$. Dark and light gray points represent convergence to target period-τ orbit and coexisting period-6τ one, respectively. (a) and (b) are obtained around initial conditions pointed by arrow in left side and right side in Fig. 2(a), respectively. (c) displays enlargement of boundaries within rectangular area in (b).

The disturbance is additionally given to a selected initial condition. The selection of an initial condition is based on the results in the preceding section. The results suggest the possibility of the convergence to other orbits different from targets. The results consequently reflect the global dynamics in function space. The clustering and scattering distribution of initial conditions toward coexisting orbits in the (σ_0,K) planes is directly connected to the sensitivity of dependence on initial conditions.

First, we discuss the domain of attraction in the two-well Duffing system with velocity feedback control. The initial condition pointed by arrow in the left side of Fig. 2(a) lies apart from initial conditions toward coexisting orbits. This implies the pointed initial condition is not close to the boundaries of the domain of attraction. Therefore, the domain of attraction around this initial condition is quite dominant by the convergence to target orbits as shown in Fig. 5(a). On the other hand, the initial condition pointed in the right side of Fig. 2(a) lies close to initial conditions toward coexisting orbits. It suggests that the pointed initial condition is located near the boundaries between the domain of attraction for target orbits and for coexisting ones. Thus, the domain of attraction around this initial condition is found to have clear boundaries as shown in Fig. 5(b).

Here we concentrate on the boundaries of the domain of attraction. In Fig. 5(b), the boundaries smoothly curve from top right to right side. A part of the boundaries are clearly enlarged as shown in Fig. 5(c). The enlargement shows no appearance of additional boundaries. In contrast, the boundaries in Fig. 6(a) have a self-similar structure. This self-similar structure is obtained around the initial condition pointed in Fig. 2(b). The boundaries exhibit rough curves in distinction to the previous smooth case of Figs. 5(b) and 5(c). More precisely, many fine striped structures are observed along each boundary. The self-similarity of the boundaries is confirmed by enlarging the fine stripes. When one enlarges a part of the stripes, the same fine stripes appear again, as shown in Fig. 6(b). When one enlarges a part of the enlargement, the same structures can be found, as displayed in Fig. 6(c). In general, self-similar structures are yielded in the phase space of chaotic dynamical systems. The crucial difference is that the domain of attraction is here defined in function space apart from the target orbits. More precisely, the $(\mu,\|\boldsymbol{\varepsilon}(t)\|_\tau)$ spaces represent the domain of attraction around the selected initial condition along temporal axis. The self-similarity in the $(\mu,\|\boldsymbol{\varepsilon}(t)\|_\tau)$ spaces implies the sensitive dependence of stabilized states on intensity and timing of small external disturbance to the selected initial condition. It implies that the controlled system loses the robustness for the initial condition. Then the global structure governing the system cannot be simple in function space.

Figure 7 shows a self-similar structure in the two-well Duffing system with displacement feedback control at $(\delta,A)=(0.46,0.4)$. This structure is obtained around the initial condition pointed by the arrow in Fig. 3. Many fine

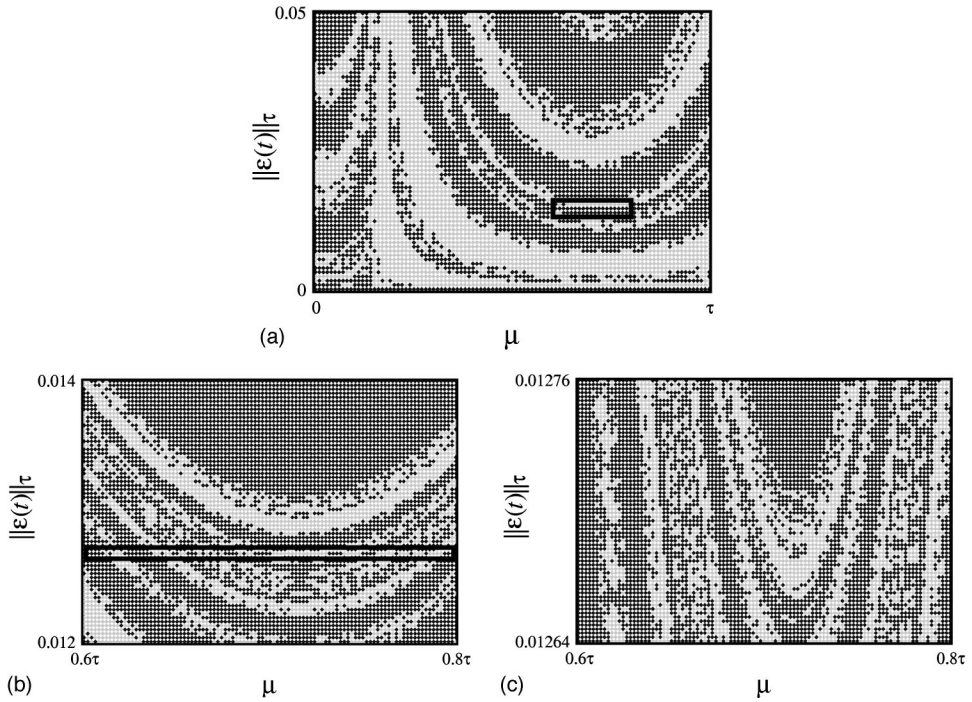

FIG. 6. Domain of attraction on $(\mu, \|\boldsymbol{\varepsilon}(t)\|_\tau)$ space in two-well Duffing system with velocity feedback control at $(\delta, A) = (0.16, 0.27)$. Dark and light gray points represent convergence to target period-τ orbit and coexisting period-6τ one, respectively. (b) and (c) are enlargement of rectangular areas in (a) and (b), respectively. They show self-similar structures around initial condition pointed by arrow in Fig. 2(b).

stripes are found along the boundaries from lower left to right side in Fig. 7(a). The enlargement of a part of the stripes displays fine striped structures again, as shown in Fig. 7(b). On the other hand, the difference from the previous case is that smooth boundaries are partly observed in the upper left of Fig. 7(a). The enlargement also shows more smooth boundaries than the previous rough case of Fig. 6. It seems that the self-similarity is truncated or localized in function space.

Figure 8 represents a self-similar structure in the Duffing system with velocity feedback control. The self-similar structure is found around the initial condition pointed by arrow in Fig. 4. The difference from the previous two cases is that there are all four types of initial conditions. Dark and light gray points represent initial conditions toward one of the target orbits and one of the coexisting orbits, respectively. Among additional two middle tones, dark and light gray points show the initial conditions toward the other target and coexisting orbit, respectively. These four types of initial conditions are spread from left to right side in Fig. 8(a). Besides, the four types are mixed with one another. The mixed structure is also observed in the upper right corner. It is clearly shown that the mixed structure is sandwiched by many layers of dark and light gray points. When a part of the mixed structure is enlarged, the same structures can be observed, as shown in Fig. 8(b). The enlargements are sandwiched between dark and light gray layers again. In this case, tangles of the domains of attraction corresponding to the four types of solutions are intrinsic in function space.

The above self-similar structures reveal that the convergence to target orbits sensitively depends on initial condition

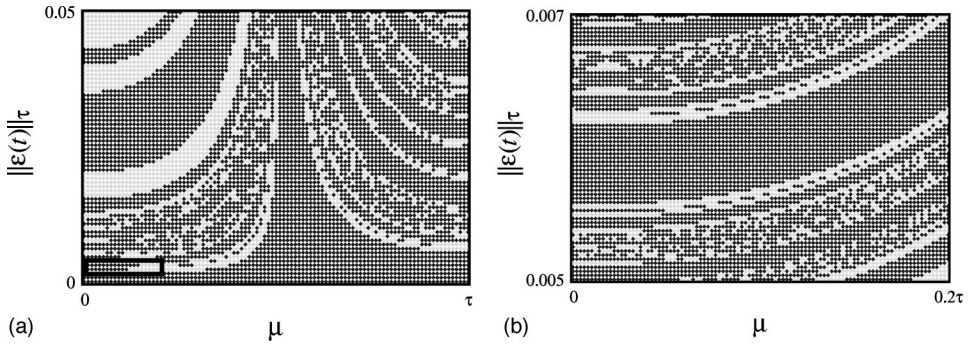

FIG. 7. Domain of attraction on $(\mu, \|\boldsymbol{\varepsilon}(t)\|_\tau)$-space in two-well Duffing system with displacement feedback control at $(\delta, A) = (0.46, 0.4)$. Dark and light gray points represent convergence to target period-τ orbit and coexisting period-6τ one, respectively. (b) is enlargement of rectangular area in (a). They display self-similar structures around initial condition pointed by arrow in Fig. 3.

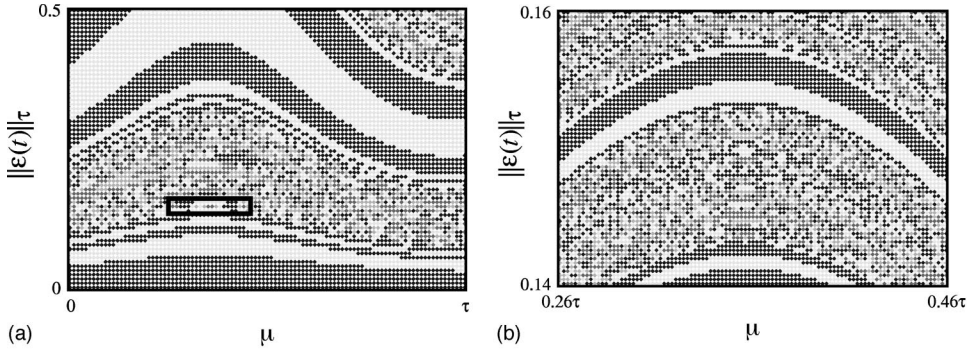

FIG. 8. Domain of attraction on $(\mu,\|\boldsymbol{\varepsilon}(t)\|_\tau)$ space in Duffing system with velocity feedback control at $(\delta,A)=(0.1,13.3)$. Dark and light gray points represent convergence to one of target period-τ orbits and one of coexisting period-3τ orbits, respectively. Among middle tones, dark and light gray points show the other target orbit and coexisting one, respectively. (b) is enlargement of (a). They show self-similar structures around initial condition pointed by arrow in Fig. 4.

in function space. In other words, successful prediction of controlling chaos is difficult before the control is achieved. It is clearly understood that this unpredictability is a disadvantage for engineering use of the control method. However, no detailed discussion for the characteristics has been obtained.

Note that we have not considered selective stabilization of two symmetric target orbits in the foregoing discussion. However, the selective stabilization is important for engineering use. Here we apply the same approach to the domain of attraction for each target orbit. Figure 9(a) is a (σ_0,K) plane in the two-well Duffing system with displacement feedback control at $(\delta,A)=(0.16,0.27)$. The classification of tones distinguishes the convergence to the two symmetric target orbits with additional dark tone. In Fig. 9(a), one clearly recognizes that initial conditions toward the two symmetric target orbits are mixed in $0.48\lesssim K\lesssim 0.7$. Correspondingly, the domain of attraction exhibits a mixed structure, as shown in Fig. 9(b). The same mixed structure holds even in the enlargement shown in Fig. 9(c). The mixed structure is here obtained close to the initial condition pointed in Fig.

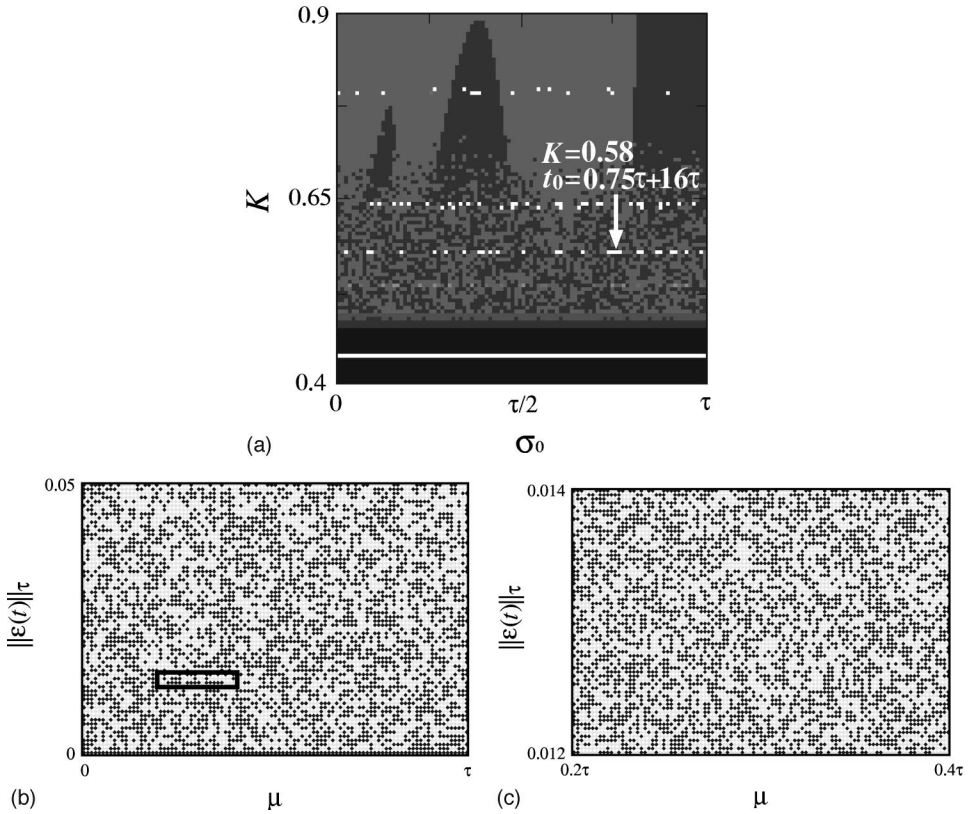

FIG. 9. Classification of stabilized orbits (a) and domain of attraction [(b) and (c)] in two-well Duffing system with displacement feedback control at $(\delta,A)=(0.16,0.27)$. In (a), classification distinguishes two symmetric target orbits with additional dark tone. (b) is obtained around initial condition pointed by arrow in (a). (c) displays enlargement of rectangular area in (a). (b) and (c) show stabilized states almost randomly alternate between each target orbit by external disturbance.

9(a). However, one easily observes the structure covers the whole onset time of control in the (σ_0, K) plane. Therefore, it is inevitable that the stabilized states almost randomly alternate between each target orbit with onset timing of control or influence of external disturbance [21]. In other words, the targeting scheme based on linearization has no possibility of effective convergence.

In this section, the domain of attraction in function space has been discussed. The results indicate complicated global structure of phase space in function space. It should be mentioned that these complicated structures are substantially induced by applying the control method to the Duffing systems. This is because all the parameters used in this paper are selected from the regions where the basins of attractions of the chaotic attractors have simple structures with smooth boundaries before onset time of control, if the uncontrolled systems have multistability.

Furthermore, we need to emphasize one inevitably remarks global dynamics of controlled systems. This is because the exact model of controlled objects is often unknown in practical systems. Then one possibly starts the control apart from the neighborhood of the target orbits. However, it obviously goes beyond the scope of linearization technique.

V. CONCLUSION

In this paper, we numerically discussed the domain of attraction for the target unstable periodic orbits in the time delayed feedback controlled Duffing systems. The approach is completely far from local stability analysis of the target orbits. The approach is directly related to the application of the control method to practical systems; decision of onset time control, and estimation of influence of noise. The numerical results reveal complicated global dynamics in function space, as opposite to clear results expected from linearization. The domain of attraction with self-similarity suggests that the success of the control sensitively depends on onset timing of control and disturbance on controlled systems. In addition, another quite complicated structure implies that the targeting scheme based on linearization does not perform effectively. We need to emphasize that the domain of attraction with self-similarity is not restricted within particular implementation of the control method or specific controlled objects. Therefore, further extension of the control method should be established in the light of the global structure in function space.

[1] *Handbook of Chaos Control*, edited by H. G. Schuster (Wiley-VCH, Weinheim, 1999).

[2] E. Ott, C. Grebogi, and A. Yorke, Phys. Rev. Lett. **64**, 1196 (1990).

[3] K. Pyragas, Phys. Lett. A **170**, 421 (1992).

[4] K. Pyragas and A. Tamaševičius, Phys. Lett. A **180**, 99 (1993).

[5] S. Bielawski, D. Derozier, and P. Glorieux, Phys. Rev. E **49**, R971 (1994).

[6] T. Hikihara and T. Kawagoshi, Phys. Lett. A **211**, 29 (1996).

[7] P. Parmananda, R. Madrigal, M. Rivera, L. Nyikos, I.Z. Kiss, and V. Gáspár, Phys. Rev. E **59**, 5266 (1999).

[8] W. Just, E. Reibold, K. Kacperski, P. Fronczak, J.A. Holyst, and H. Benner, Phys. Rev. E **61**, 5045 (2000).

[9] J.E.S. Socolar, D.W. Sukow, and D.J. Gauthier, Phys. Rev. E **50**, 3245 (1994).

[10] T. Ushio, IEEE Trans. Circuits Syst., I: Fundam. Theory Appl. **43**, 815 (1996).

[11] H. Nakajima and Y. Ueda, Physica D **111**, 143 (1998).

[12] W. Just, T. Bernard, M. Ostheimer, E. Reibold, and H. Benner, Phys. Rev. Lett. **78**, 203 (1997).

[13] K. Pyragas, Phys. Rev. Lett. **86**, 2265 (2001).

[14] J.K. Hale, *Theory of Functional Differential Equations* (Springer-Verlag, New York, 1977).

[15] F.C. Moon and P.J. Holmes, J. Sound Vib. **65**, 275 (1979).

[16] Y. Ueda, Chaos, Solitons Fractals **1**, 199 (1991).

[17] G. Duffing, *Erwungene Schwingungen bei veränderlicher Eigenfrequenz und ihre technische Bedeutung* (Druck und Verlag von Friedr. Vieweg & Sohn, Braunschweig, 1918).

[18] Y. Ueda, H. Nakajima, T. Hikihara, and H.B. Stewart, in *Dynamical Systems Approaches to Nonlinear Problems in Systems and Circuits*, edited by Fathi M. A. Salam and Mark L. Levi (SIAM, Philadelphia, 1988), pp. 128–137.

[19] T. Hikihara and Y. Ueda, Chaos **9**, 887 (1999).

[20] H. Nakajima, Phys. Lett. A **232**, 207 (1997).

[21] The similar result has been reported in connection with systems with chaotic saddle. See T. Kapitaniak, Chaos, Solitons Fractals **12**, 2363 (2001).